PCCP

PAPER

View Article Online
View Journal

Cite this: DOI: 10.1039/d5cp03957f

Modelling the adsorption of partially aminated dendrimer monolayers

Jason Palin, [a] Christopher J. Barrett, [bc] Ozzy Mermut [c] and Neal Madras *[d]

Received 14th October 2025,
Accepted 6th June 2026

DOI: 10.1039/d5cp03957f

rsc.li/pccp

We develop two modifications of the Random Sequential Adsorption (RSA) model for capturing the adsorption kinetics and final surface layer geometry of partially aminated dendrimers. These modified models incorporate several of the features which distinguish the adsorption behaviour of partially aminated dendrimers from that of previously studied dendrimers with a homogenously distributed charge. In the first modification, dendrimer shaped objects are placed with the intersection between attempted placements and existing placements being checked only at a certain fraction of end groups. In the second, disks are placed with an effective radius representing electrostatic repulsion effects but are also able to overlap up to a specified degree. These models are applied towards interpretation of experimental adsorption results of a recent dendrimer of interest, dendritic polyglycerol amine (dPGA).

1. Introduction

Dendrimers are a relatively novel class of synthetic polymers characterized by a highly symmetric spherical shape and a highly regular branching pattern.[1] The high degree of control over their architecture and properties has led to a variety of biomedical and pharmaceutical applications.[2,3] Charged dendrimers such as poly(propylene imine) (PPI) and poly(amido amine) (PAMAM) have been of particular recent interest because of the presence of amine groups facilitating adsorption of dendrimers in solution to charged surfaces.[4] Theoretical work characterizing the adsorption kinetics and final surface layer of charged dendrimers has been done with these dendrimers specifically in focus.[5] In this paper, techniques are developed and applied to characterize another charged dendrimer – dendritic polyglycerol amine (dPGA) – a novel dendrimer which has attracted interest for its high performance as a substrate for the growth of neural cell culture.[6–8] Similar to PPI and PAMAM, dPGA contains amine groups which facilitate adsorption when placed in solution. It is distinct, however, in the important respect that amine groups are present only as a (controlled) fraction of some branch-ends of the dendrimer. Previous models of charged dendrimer adsorption approximate adsorbed molecules as disks with a homogenously distributed charge exerting a coulombic force on other molecules.[5,9] These models can accurately reproduce patterns from AFM images of adsorbed PAMAM dendrimers, but are no longer accurate for AFM images of adsorbed dPGA which are qualitatively different. Moreover, while the charge of each molecule can be adjusted in these models, there is no parameter specific enough to describe the fraction of branch-end amination which is of interest in dPGA. In this paper, two variations of the Random Sequential Adsorption (RSA) simulation model for polymer adsorption are introduced and applied to experimental results for dPGA. The first of these variations involves placing dendrimer shaped objects on a surface sequentially with an adsorption mechanism concentrating on a specified fraction of branch ends, which can then be controlled to simulate the influence of varying fractions on the adsorption kinetics. The second variation simulates placement of individual molecules where overlapping molecules are allowed to intersect up to a certain degree and non-overlapping molecules feel electrostatic repulsion from each other. This allows for a qualitative reproduction of the adsorption pattern observed from AFM images, and quantitatively is able to provide a very strong fit to experimental pair correlation functions.

2. Experimental methods

2.1. Materials

dPGA (DendroTEK Biosciences[6–8]) solutions were prepared with ~550 kDa dPGA and pH 7.4 (1×) PBS to a concentration of 50 μg mL^{-1} unless indicated otherwise. Solutions used for cell culture were filtered through a 0.22 μm filter to ensure sterility. For ellipsometry measurements to determine layer thickness,[8] silicon wafers were obtained from Alpha Nanotech (ultra-flat 4″ single-sided silicon wafers, grade prime/CZ virgin, type/dopant

[a] School of Physics and Astronomy, University of Leeds, Leeds, LS2 9JT, UK
[b] Department of Chemistry, McGill University, Montreal, QC, H3A 2K6, Canada
[c] Department of Physics and Astronomy, York University, Toronto, ON, M3J 1P3, Canada
[d] Department of Mathematics and Statistics, York University, Toronto, ON, M3J 1P3, Canada. E-mail: madras@yorku.ca

P/Boron, orientation ⟨100⟩, thickness 525 μm ± 10 μm, resistivity 1–30 Ohm cm) and were cleaved into approximately 1 × 4 cm pieces and rinsed with deionized water prior to being dipped into solutions. For AFM analysis, silicon wafers were used from Virginia semiconductor (diameter 50.8 mm ± 0.3 mm, orientation ⟨100⟩ ± 0.5°), dopant boron/P type, resist <0.01 Ohm cm, material Cz, pri. Flat 15.88 ± 1.65 mm ⟨110⟩ ± 0.5, thickness 525 μm ± 25 μm, surface single side polished backside etched, were cleaved into approximately 1 × 4 cm pieces then cleaned with piranha solution and stored in Milli-Q water prior to depositing films.

2.2. Sample preparation

As detailed experimentally previously,[8] for layers on silicon a 50 μg mL^{-1} dPGA solution was prepared in PBS, pH 7.4. The silicon wafer was then submersed, by hand, for a set amount of time. Following adsorption, the wafer was then briefly rinsed with deionized water followed by drying by a stream of air prior to any characterization. For layers on colloids; a 40 mL solution of 0.5 mg mL^{-1} dPGA prepared in PBS (pH 7.4) was prepared. To this, 0.5 mL (approximately 200 mg) of the Snowtex suspension was pipetted followed by sonication and vortex. The solution was left to mix overnight after which the solution was centrifuged at 4700 rpm. The supernatant was then removed to remove any un-adsorbed polyelectrolyte from the colloids. To the pellet, 40 mL PBS (pH 7.4) was added. The sample was sonicated and vortexed until the pellet was re-dispersed completely and was then left to stand for at least 30 min. A total of three washings were performed. Samples were dried overnight under vacuum at 100 °C for further characterization.

2.3. Ellipsometry

Ellipsometry measurements were performed on a Gaertner ellipsometer at 633 nm under ambient humidity and room temperature.[8] The software used for thickness calculations was the Gaertner Ellipsometer Measurement Program, version 2023 upgrade. Samples were allowed to air dry until water was no longer visible on the surface before taking measurements. A series of six measurements were taken at different positions on the film from which a mean thickness and standard deviation could be calculated. The model used to fit the data included an oxide layer with refractive index of 1.46 and thickness of 14 Å for the silicon used for AFM or 40 Å for the silicon used for dipping with a polymer layer on top with a fixed refractive index of 1.45. In the model, the variable being calculated was the thickness of the top layer with an input estimate of 100 Å.

2.4. Atomic force microscopy (AFM)

AFM scans were obtained using an Asylum Research MFP-3D AFM operating at room temperature and ambient humidity in AC Air mode.[8] An ACTA probe with a nominal resonance frequency of 300 kHz and nominal spring constant of 40 N m^{-1} from AppNano was used in tapping mode in air. Samples were prepared on a silicon substrate, which was attached to a glass microscopy slide using double sided adhesive tape prior to scanning. Scans were performed at a rate of 1 Hz with the setpoint, integral gain, and drive amplitude adjusted to improve tracking and scan quality for each sample. Roughness values R_q and R_a (average roughness and root mean square roughness, respectively) were extracted from scans after processing to remove tilt and curvature using Asylum Research software version 16.10.211 Igor Pro 6.38B01 software. Scans were processed into the image (*e.g.* Fig. 1) using Gwyddion 2.65 software.

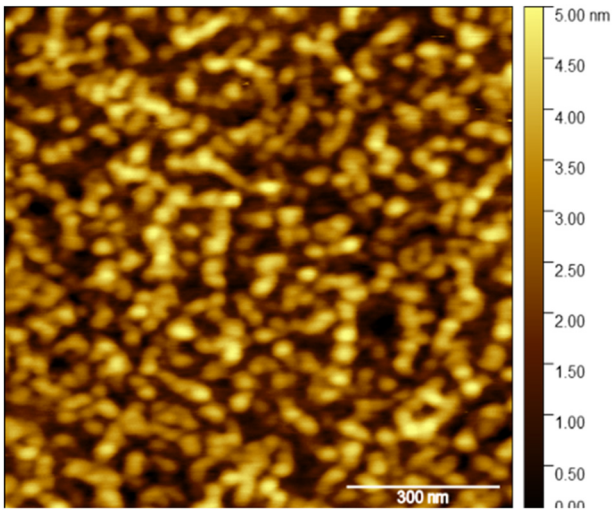

Fig. 1 Representative 1 μm AFM image of a 550 kDa dPGA monolayer after 30 s of adsorption time. Adapted from ref. 8 Fig. 3 with permission from The American Chemical Society.

3. Random sequential adsorption modelling

3.1. The basic Random Sequential Adsorption model

To model the adsorption behaviour of dPGA, two different Random Sequential Adsorption (RSA) models were used to capture the kinetics of the adsorption process and the pattern of the final adsorbed monolayer. The basic RSA model coarsely simulates the adsorption kinetics of individual colloidal particles *via* a simple Monte Carlo algorithm.[10] In each step of the algorithm, an "attempt particle" is created at a random location on a surface of some specified size and geometry. If this attempt particle intersects with an already placed particle, it is discarded. If it does not intersect with any of the already placed particles, it becomes placed itself (see Fig. 2). This basic algorithm has been generalized to different shapes of placed particles[11] and placements of basic polymer structures.[12] A typical 2-dimensional RSA simulation yields two basic quantities of interest. The first is the coverage fraction Θ at any time of the simulation process, defined by

$$\Theta = N(A_p/S) \quad (1)$$

where N is the number of placed particles, A_p is the area of each particle and S is the size of the total surface the particles are placed on. Θ is typically expressed as a function of the amount of placement attempts τ by computing Θ after each attempt. In

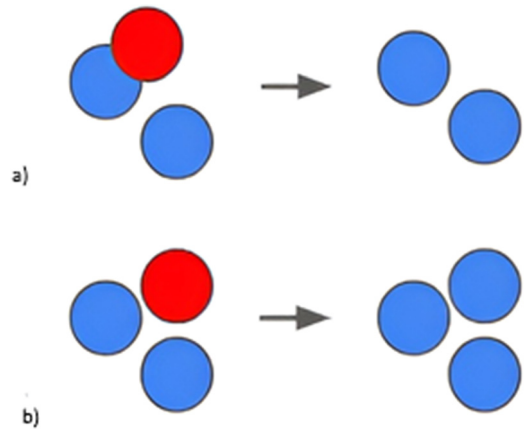

Fig. 2 Illustration of a time step in a basic RSA process, where each disk represents a particular molecule. In (a), the red attempt particle intersects with the blue placed particles and is rejected. In (b), it is free of intersection and becomes placed.

the case of RSA with circular disks, a variety of approximations and analytic expressions are known for $\Theta(\tau)$.[13] The second quantity of interest is the jamming coverage, defined as the value of Θ when no more successful particle placement attempts are possible. For RSA of circular disks this is known to be 0.547.[11] The jamming coverage gives a measure of the "optimal" surface coverage for randomly placed particles of a given geometry; when actual particles fail to obtain the jamming coverage, it indicates the presence of effects determining adsorption kinetics beyond solely the exclusion of intersecting particles. An inherent limitation of the RSA approach, including our modifications below, is that it does not include dynamics of adsorbed particles such as diffusion, rearrangement, or conformational relaxation. In that sense, an RSA model is mainly a phenomenological description and not a theoretical prediction.

3.2. Heterogeneous dendrimer RSA model

For dPGA, it is convenient for several reasons to use a modification of the basic RSA model specifically for heterogeneous dendrimers such as dPGA. The dPGA structure consists of a hyperbranched polyglycerol structure with some fraction of the ends of branches replaced by amine groups, which provide the main mechanism of adsorption of dPGA molecules to a negatively charged cell membrane.[6]

This motivates the following modifications to the basic RSA algorithm: instead of placing single particles, we place all of the dendrimer shaped objects, and instead of checking for intersection between any part of the attempt molecule with already placed dendrimers, we check it specifically at a specified fraction of branch ends. In more detail, the algorithm is as follows:

dPGA-RSA algorithm:

1. A single disk, representing the core of the dendrimer, is placed at a random location on the surface.

2. Three random angles are chosen, and three more disks are attached to the core disk from step 1.

3. For each of the three disks attached in step 2, two random angles are chosen and two disks are attached.

4. Step 3 is repeated $g - 1$ more times, where g is the chosen number of generations, with respect to the most recent attached generation of disks.

5. A set fraction K of the outermost disks are selected as "B-disks".

6. If any of the selected B-disks intersect with any disk of previously placed dendrimers, the attempt dendrimer is rejected and we return to step 1. If not, then the attempt dendrimer becomes placed, and we return to step 1.

Hence, at each step a dendrimer shaped object is built at a random location on the surface, and we check for intersection with existing dendrimers only at a specified fraction of beads located at branch-ends (see Fig. 3). There are two main benefits for this particular modified RSA model. Firstly, models for RSA of other charged dendrimers (*e.g.* PAMAM dendrimers[5,9]) place single disks as in a typical RSA simulation, but with an increased effective radius calculated by a screened coulombic force from the charge of each dendrimer. However, unlike in PAMAM dendrimers the charges in dPGA are not uniformly distributed throughout the dendrimer, and moreover the fraction of aminated end group is a controlled variable in the synthesis of dPGA, making it particularly useful to have the charged end groups as a tuneable parameter.

Secondly, the jamming coverage for dPGA RSA is significantly lower than that of single bead RSA, and hence can be matched to actual measures of surface coverage for dPGA from experiment. Jamming coverages for the dPGA-RSA algorithm with 50% B-disk fraction ranged between 0.3 and 0.4 for low generation numbers (note the coverage fraction is computed as the fraction of the surface covered by dendrimers, hence dendrimers which overlap are not double-counted). The

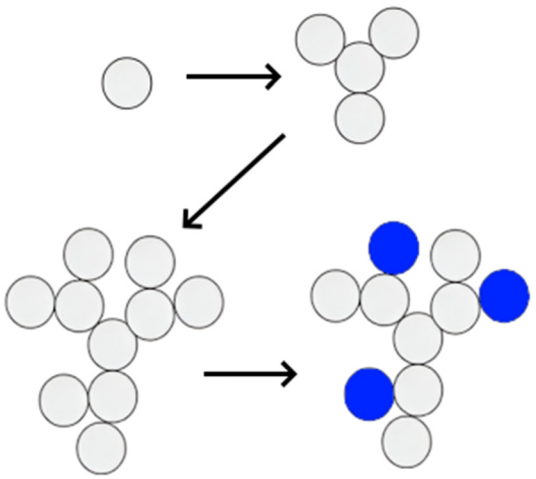

Fig. 3 The dendrimer construction process from the dPGA-RSA algorithm: a single disk is placed randomly, 3 disks are attached at random angles, two disks are attached to the most recently placed disks until the desired number of generations is reached, and then a certain fraction of disks at the ends of branches are selected to be B-disks (blue). Here the entire collection of disks represents a single dendrimer.

approach, hence, perhaps coincides better with what is likely to be a real physical adsorption process of dendrimers than the basic RSA model, although it shares several of the same limitations such as a lack of detailed conformational information, intermolecular interaction, or surface re-arrangement dynamics, as adsorption in the RSA model is treated as a fixed and irreversible process. To compare the results of the dPGA-RSA algorithm with experimental results, image analysis of single-layer RSA AFM was performed for an estimate of the surface coverage fraction. Depending on the exact threshold and image used, coverage fractions ranged between 0.25 and 0.40. Since the adsorbed dendrimer formed a monolayer, the ellipsometry film thickness data over time (which averages over areas of the surface with and without the adsorbent) can be assumed to be roughly proportional to the surface coverage over time. Then by normalizing the ellipsometry data to obtain a sequence of points with the maximum value equal to the surface coverage fraction of 1-hour AFM images, we obtain surface coverage data to which dPGA-RSA simulation can be compared.

In Fig. 4a the ellipsometry data have been normalized to have a maximum value of 0.3 and are plotted along with a dPGA-RSA fit of 4 generation dendrimers with 50% B-disk fraction being placed at a rate of 20 dendrimers/second. The RSA data coincide well with experiment for early times and for final surface coverage, but gradually slow at times in between whereas the experimental coverage keeps increasing rapidly and then slows more drastically. This suggests the importance of shifting effects on the surface in the adsorption process, which RSA methods do not capture. At low surface coverage, adsorbing dPGA molecules are able to 'make space' for themselves by pushing/repelling other molecules. When the surface coverage becomes high enough to make this pushing difficult due to crowding effects, the lack of available surface effects becomes more important and the adsorption rate drops quickly. Further work is required to describe the specific physical mechanisms driving this surface rearrangement process; the level of coarse-graining of RSA means that it provides limited information on intermolecular dynamics during the adsorption process.

Another use of the dPGA-RSA simulation is to extrapolate the adsorption kinetics to those of dPGA molecules with different branch-end amination fractions. In Fig. 4b 50% B-disk fraction RSA fit to experimental results (as in Fig. 4a) is repeated with B-disk fractions of 25% and 75%. Unsurprisingly, the surface coverage functions of varying fractions do not differ at early times and low surface coverage, and begin to spread at higher coverages according to how many branch-ends must be free of intersection in order to adsorb successfully.

3.3. Adsorption monolayer analysis

AFM images of PAMAM dendrimers,[5,9,14] another class of charged dendrimers, show that individual molecule sized particles spread out from each other. In contrast to this, AFM images of dPGA as in Fig. 6a show an abnormal pattern where isolated individual molecule sized particles appear alongside

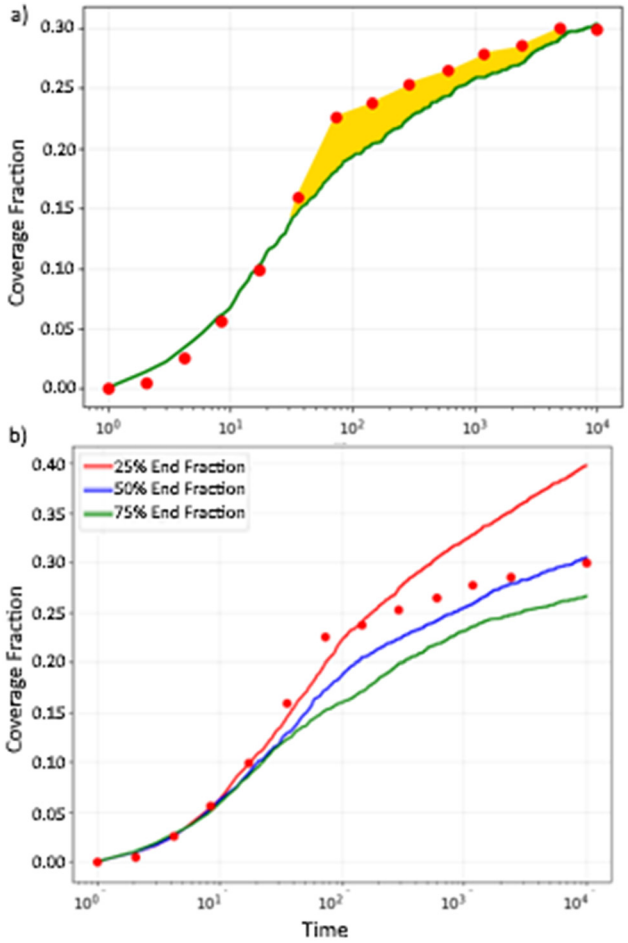

Fig. 4 (a) Normalized ellipsometry data (red points) plotted along with a 4 generation dendrimer dPGA-RSA simulation, with the deviation between simulation and experiment highlighted in yellow. Dendrimers have a 50% B-disk fraction and are placed at a rate of 20 per time step. (b) dPGA-RSA simulation with the same parameters as in Fig. 4a, but with varying fractions K = 0.25, 0.5, and 0.75 of B-disks. Experimental data in both figures were taken from data originally published in ref. 8.

larger irregularly shaped blobs of several molecules. This can be partially explained by the fact that dPGA molecules are less highly charged (with amination occurring only at a certain fraction of end groups) compared to PAMAM dendrimers, so electrostatic repulsion effects are less prominent. However, weaker electrostatic repulsion alone would still produce a layer of isolated individual molecules, which are only more tightly packed together.

To characterize the combination of clustered and unclustered molecules in the adsorption layer of dPGA, we shall employ another RSA model which includes both electrostatic repulsion and allowance for partial intersection of molecules. Before this, we analyse the AFM images to determine parameters for the size of each molecule and the extent of intersection that occurs between molecules. To estimate the average size of an individual molecule, we firstly compute the size of all connected components of the adsorbent (in Fig. 6a these connected components are the individual red spots). The

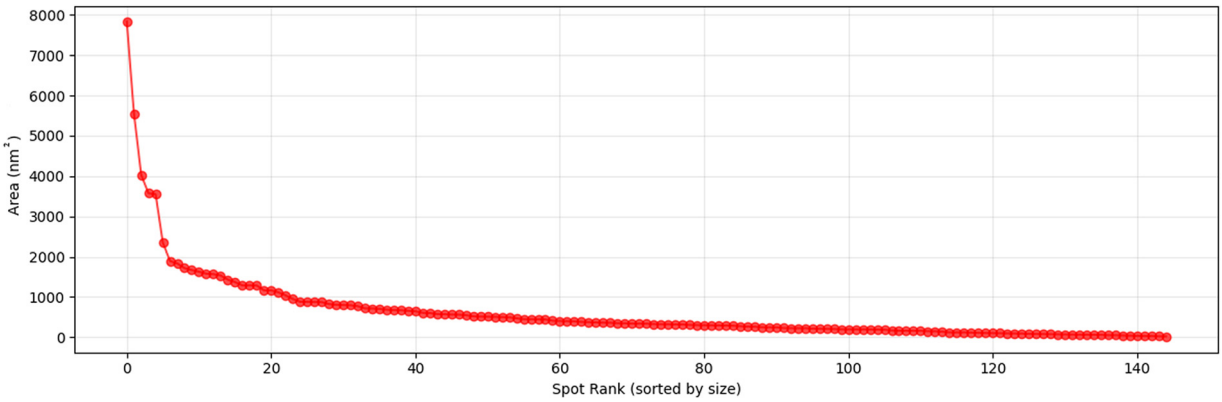

Fig. 5 Areas of the connected regions of adsorbent from the AFM image in Fig. 1 with the x-axis an indexing of these regions ordered by decreasing size.

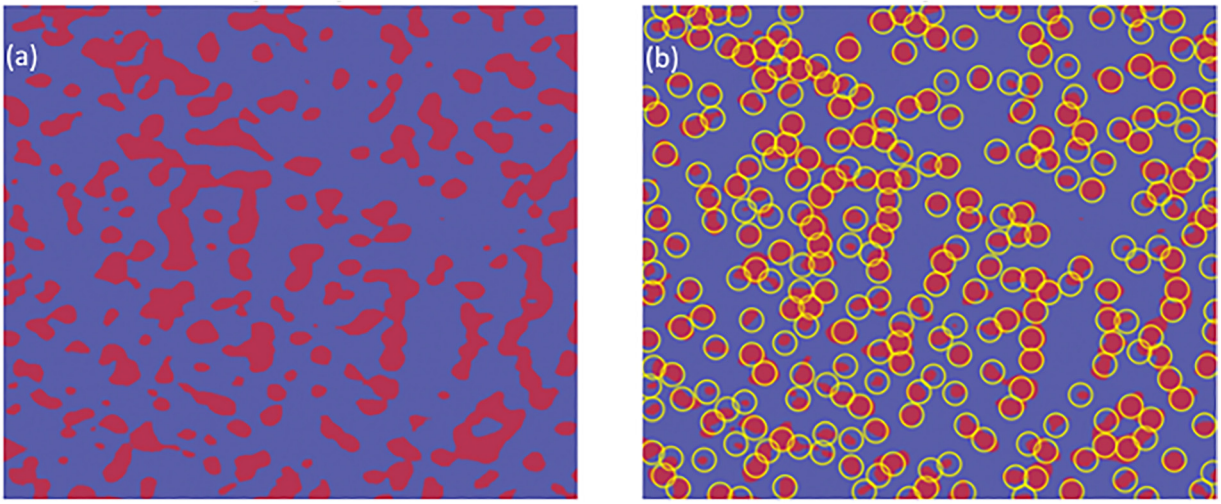

Fig. 6 (a) AFM image of adsorbed 550 kDA after a 30 s adsorption time. The red spots indicate areas of the AFM image that were above a height threshold, and the blue background indicates areas of the AFM image which fell below the threshold. (b) The AFM image of (a) fit with circles using the estimated radius of $\approx$20 nm and a maximum intersection fraction of 0.25. Each circle here represents a single dendrimer.

distribution of areas among these connected components is shown in Fig. 5. Our code labelled each individual component by its area. Then, by inspection, we filtered out areas of components in the higher end of the distribution which clearly appeared to represent clusters of several molecules as well as the smallest components at the bottom end of the distribution which are artifacts of the threshold. Then an average of the remaining areas can be taken to obtain an estimate of the average area of an individual adsorbed molecule. In this manner the areas of the distribution between $\approx$595 nm^2 and $\approx$2691 nm^2 were used to yield an estimated average area of approximately 1224 nm^2, with a high standard deviation of 501.152 nm^2. Assuming that the mean shape of adsorbed molecules is circular, this suggests the average diameter of a particle is about 39.5 nm, in line with previous estimates of the adsorbed diameter of dPGA.[6] Varying the exact upper and lower thresholds on the order of several 100 nm^2 led to diameters in the range of 37–42 nm, which are still in agreement with previous estimates and do not have a significant impact on the simulation statistics such as cluster size as described below.

Next, to calculate the degree of intersection between adsorbed molecules as well as to visualize individual particles, an algorithm was developed to "fit" or cover the adsorbent in AFM images with circles. The uncovered area above the height threshold was randomly sampled, circles with a radius based on the above estimates were placed at each sampled point, and the circle which covered the highest fraction of threshold area was placed and the others rejected. We note that coverage here, and in the simulations described below, is computed as the amount of covered area, so overlapping particles are not double-counted. The placed circles were allowed to intersect with each other up to a certain fraction P of their area. To calculate the optimal (with respect to accurate coverage) value of P, a reward function

$$F(C(P)) = C_r(C) - \frac{T_o}{T_a}(C) \quad (2)$$

was maximized for different trial values of P, where C denotes the set of circles being used to cover the image, C_r the fraction of red pixels covered, T_a the total red area, and T_o the total area of overlap between circles. Optimal values of P for different images ranged between 0.2 and 0.3.

To explore the magnitude of the effects determining the clustered–unclustered pattern of the final adsorption layer, another RSA algorithm was employed which accounted for both electrostatic repulsion between separated molecules and attraction due to van der Waals forces between intersecting molecules. In this algorithm, which we hereafter refer to as EA-RSA, single circular disks (representing individual dPGA molecules) of a fixed radius R are placed sequentially at random locations on a surface as in the basic RSA algorithm. However, the criterion for a successful placement attempt is modified. We associate the parameter $J \geq R$ to all disks to represent a repulsive electrostatic field, and a parameter $K \in [0,1]$ which gives the maximum allowable intersection between two disks. The rules for an attempt disk to be successfully placed are as follows:

EA-RSA successful placement criteria

1. If an attempt disk intersects with any already placed disk by a higher fraction of its total area than K, it is rejected.

2. If an attempt disk does not intersect with any already placed disk, but has distance (measured from its centre to the edge of any other disk) less than J to any already placed disk, it is rejected.

3. Otherwise, the attempt disk becomes a placed disk.

Hence, colloquially, disks are allowed to intersect with each other up to a fraction K, and if a disk does not intersect with any already placed disks, it must be a distance of at least J from any point in all placed disks.

The radius R of each disk was set at approximately 20 nm based on the estimate for the average obtained above. The parameter K was set to 0.25 based on the coverage optimized value of P obtained above. This suggests a large degree of molecular overlap is possible, which we speculate is made possible by the large size and randomly branched nature of dPGA enabling significant conformational flexibility and interpenetration in response to attractive van der Waals forces. The value of J was then treated as a model parameter and was then fit to minimize the mean squared error (MSE) between the pair correlation function of the EA-RSA simulation output and the pair correlation function of actual AFM images. This yielded an optimal value of $J = 27.024 = 1.35R$. The MSE, which was calculated for 50 uniformly spaced points between $r = 0$ and $r = 100$, was 0.04279 with a standard deviation of 0.00657 over 20 simulation runs with this parameter. An example of the final adsorption monolayer produced by the EA-RSA algorithm is displayed in Fig. 7. As the final layer here represents equilibrated adsorption behaviour, the parameter J gives an estimate of the effective range of interaction, hypothesized to be primarily repulsive electrostatic interaction, between dPGA dendrimers. Comparison of this estimate to relevant quantities such as the typical interaction range or Debye length for dPGA or other large charged dendrimers requires further experimental or theoretical advances.

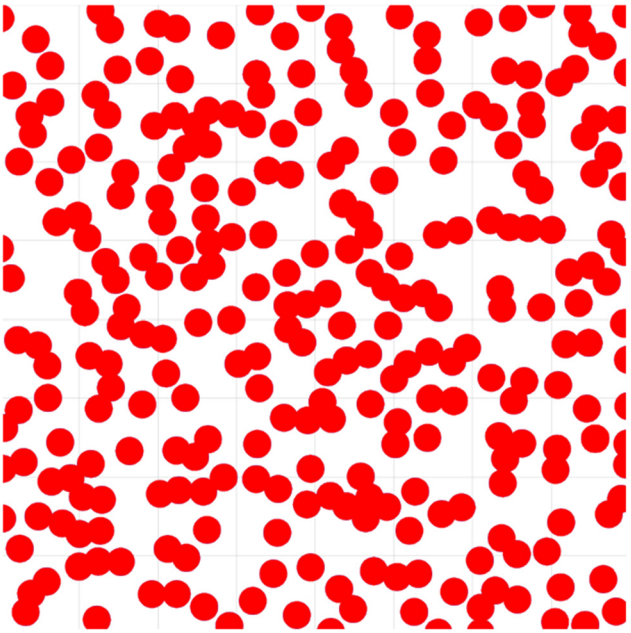

Fig. 7 Visualized output of a simulation run of the EA-RSA algorithm, with $K = 0.25$ and $J = 27.024$.

The EA-RSA simulations were run on surfaces of the same size as the surfaces in AFM images, and terminated when the surface coverage matched AFM data. Qualitatively, the EA-RSA simulation results capture the pattern of large clusters of molecules alongside isolated individual molecules seen in the AFM data. Quantitatively, pair correlation functions (Fig. 8) for the EA-RSA simulation are remarkably close to pair correlation functions calculated from the circle fitted (Fig. 6b) AFM data. Similar magnitude peaks in the pair correlation functions occur at r values between approximately 29 and 34 nm, corresponding to the density of molecules in clustered regions. A steep dropoff then occurs as the r value increases past a distance where molecules overlap, indicating repulsive effects between molecules without intermolecular forces holding them together, and beyond this value molecular density is uncorrelated. When the electrostatic repulsion parameter J is set to zero, this peak-dropoff behaviour disappears and the pair-correlation function goes to approximately 1 as soon as the hard core repulsion (scaled by K) is exceeded (not shown). In general, increasing J causes the first spike and first trough to increase in magnitude and width and decreasing J has the opposite effect. Varying the parameter K has the effect of shifting the size and location of the first peak along the radius axis. At significantly low K (<0.15) the first peak shifts to lower r values (<30 nm) and flattens; as K approaches 1 the first peak becomes localized around J plus the radius of the circles. Values of J between approximately 25 and 29 nm did not cause significant qualitative changes from the pictured best fit, and similarly values of K between approximately 0.22 and 0.29 continued to return qualitatively similar fits.

Additionally, the cluster size distributions – the number of clusters with a given amount of particles – were computed from

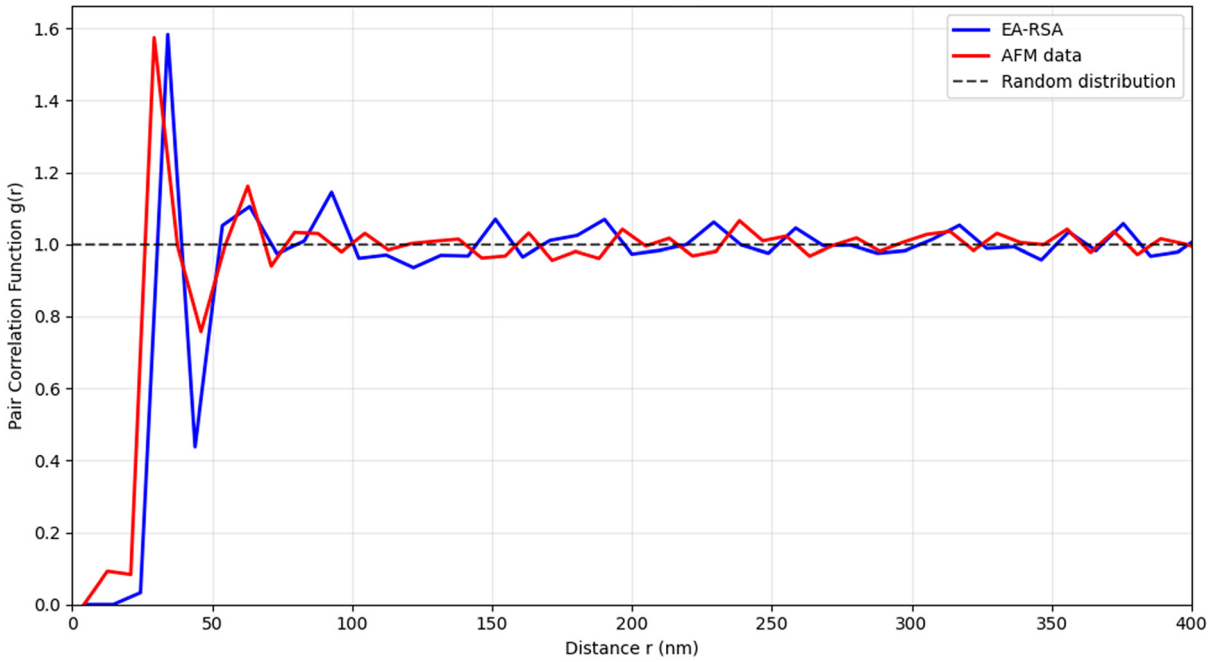

Fig. 8 Pair correlation function of EA-RSA simulation result plotted alongside the pair correlation function obtained from circle-fitted AFM data.

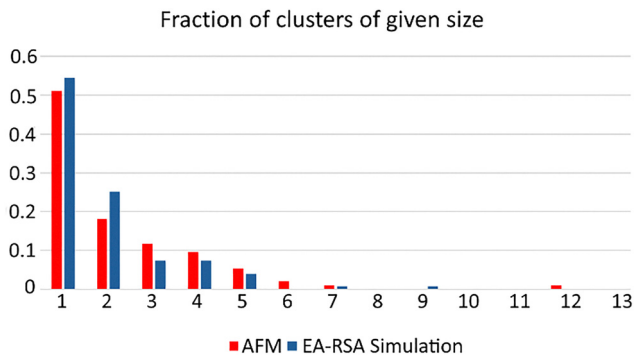

Fig. 9 The fraction of clusters for given sizes (in terms of number of particles) from the analysed AFM image in Fig. 6b and the EA-RSA simulation from Fig. 7.

the analyzed AFM image and the EA-RSA simulation and display a very strong agreement. Further simulation analysis showed that the EA-RSA distribution in Fig. 9 is representative, as Table 1 shows. Furthermore, the EA-RSA simulations were also tested with a more realistic scenario of K values being distributed over a range of plausible values, which showed strong agreement with a static K value of 0.25.

Table 1 Mean fractions of clusters from 10 EA-RSA simulations with J = 27.024 and with K = 0.25 and K uniformly distributed between 0.2 and 0.4. Brackets contain standard deviations

Cluster size	K = 0.25	K = Unif (0.2,0.4)
1	0.4979 (0.008)	0.4955 (0.036)
2	0.2372 (0.021)	0.2443 (0.032)
3	0.1229 (0.007)	0.1210 (0.026)
4	0.0661 (0.012)	0.0559 (0.007)
>4	0.0758 (0.020)	0.0836 (0.027)

4. Conclusions

Here we introduced two different Random Sequential Adsorption models to capture the time dependent surface coverage and final layer characteristics of the partially aminated dendrimer dPGA.

In the first (dPGA-RSA algorithm) model, dendrimer shaped objects were placed instead of circular disks as in the typical RSA model, and intersection was checked only at a fraction of end groups of these dendrimers. Comparison of the results of this model with ellipsometry data highlighted the effects of molecular re-arrangement on the adsorption kinetics, and also enabled the treatment of end-group amination as a model parameter.

In the second (EA-RSA) model treated here, a previously used RSA model for charged dendrimers which included an effective exclusion field around adsorbed dendrimers was modified to also allow for overlapping dendrimers to intersect up to a certain degree. The EA-RSA model was able to qualitatively capture the distinctive features of partially aminated dendrimer adsorption as seen in AFM images of adsorbed monolayers, as well as produce a very strong fit to the pair-correlation function of experimental monolayers, capturing certain features which a basic RSA simulation or typical charged dendrimer RSA simulation could not.

Author contributions

Models were designed by JP and NM with feedback and guidance from OM. Algorithms and simulations were coded

and run by JP. Experimental work was performed by the group of CJB.

Conflicts of interest

There are no conflicts to declare.

Data availability

All data supporting this research are included in the body of the article. All code used in this paper is posted in GitHub at https://github.com/jasone647/Partially-Aminated-Dendrimer-RSA-Code.

Acknowledgements

The authors are grateful to Amanpreet Parihar and Amy Praetzel of McGill University for acquiring and sharing the ellipsometry and AFM data, also supervised by Linda Reven of McGill Chemistry and Timothy Kennedy of the Montreal Neurological Institute, as well as to William Pietro of York University for a helpful discussion. The authors gratefully acknowledge research funding from the Natural Sciences and Engineering Research Council of Canada (grants DGECR RGPIN-2020-06539 to O.M. and RGPIN-2025-06291 to N.M.), the Canada Foundation for Innovation (41723, 12939), and the Canada First Research Excellence Fund (CFREF-2015-00013 and CFREF-2022-00010 to O.M.).

References

1 D. Yan, C. Gao and H. Frey, *Hyperbranched polymers: synthesis, properties, and applications*, John Wiley & Sons, 2011.
2 A. A. Chis, C. Dobrea, C. Morgovan, A. M. Arseniu, L. L. Rus, A. Butaca, A. M. Juncan, M. Totan, A. L. Vonica-Tincu, G. Corms, A. C. Muntean, M. L. Muresan, F. G. Gligor and A. Frum, *Molecules*, 2020, **25**, 3982.
3 F. Najafi, M. Salami-Kalajahi and H. Roghani-Mamaqani, *J. Iran. Chem. Soc.*, 2021, **18**, 503–517.
4 D. Kaur, K. Jain, N. K. Mehra, P. Kesharwani and N. K. Jain, *J. Nanopart. Res.*, 2016, **18**, 146.
5 B. P. Cahill, G. Papastavrou, G. J. Koper and M. Borkovec, *Langmuir*, 2008, **24**, 465–473.
6 J. P. Clément, L. Al-Alwan, S. D. Glasgow, A. Stolow, Y. Ding, T. Quevedo Melo, A. Khayachi, Y. Liu, M. Hellmund, R. Haag, A. J. Milnerwood, P. Grütter and T. E. Kennedy, *ASN Neuro*, 2022, **14**, 17590914211073276.
7 N. A. Uccelli, D. Chitsaz, J. D. Gothie, D. Kakkar, E. Mohammadifar, J. P. Antel, R. Haag and T. E. Kennedy, *bioRxiv*, preprint, 2025, , DOI: 10.1101/2025.06.23.661031.
8 A. Parihar, A. Praetzel, V. Toader, N. Marcal, M. Pestemalciyan, E. Mohammadifar, R. Haag, C. J. Barrett, T. E. Kennedy and L. Reven, *ACS Chem. Neurosci.*, 2025, **16**, 4511–4518.
9 M. B. Engelhardt, P. Markus, N. Helfricht and G. Papastavrou, *J. Colloid Interface Sci.*, 2025, **686**, 852–863.
10 J. Feder, Random sequential adsorption, *J. Theor. Biol.*, 1980, **87**, 237–254.
11 P. Kubala, P. Batys, J. Barbasz, P. Weroński and M. Cieśla, *Adv. Colloid Interface Sci.*, 2022, **306**, 102692.
12 M. Cieśla, *Phys. Rev. E: Stat., Nonlinear, Soft Matter Phys.*, 2013, **87**, 052401.
13 Z. Adamczyk, *Particles At Interfaces: Interactions, Deposition, Structure*, Elsevier, 2017.
14 R. Pericet-Camara, G. Papastavrou and M. Borkovec, *Langmuir*, 2004, **20**, 3264–3270.